All-optical NRZ-to-AMI conversion using linear filtering effect of silicon microring resonator

Qiang Li (李 强)[1], Tong Ye (叶 通)[1*], Yuanyuan Lu (卢媛媛)[1], Ziyang Zhang[2], Min Qiu[2], and Yikai Su (苏翼凯)[1]

[1]*State Key Laboratory of Advanced Optical Communication Systems and Networks, Department of Electronic Engineering, Shanghai Jiao Tong University, Shanghai 200240*

[2]*Department of Microelectronics and Applied Physics, Royal Institute of Technology (KTH), Electrum 229, 16440, Sweden*

[*]*E-mail: yetong@sjtu.edu.cn*

Received January 22, 2008

We experimentally demonstrate 10-Gb/s format conversion from non-return-to-zero (NRZ) to alternate-mark-inversion (AMI) using the linear filtering effect of silicon microring resonator. Our discussion and analysis in simulation further show that a 10-Gb/s AMI signal with good quality can be obtained by a resonator with a notch depth larger than 25 dB when the 3-dB bandwidth is 0.4 nm.

OCIS codes: 060.0060, 230.1150, 230.4555.

doi: 10.3788/COL20090701.0012.

All-optical clock recovery is a key technique in future all-optical communication networks. Clock recovery based on non-return-to-zero (NRZ) format data, which has been widely used for its simplicity and bandwidth efficiency, shows implementation difficulties for the lack of discrete clock components. All-optical format conversion from NRZ to alternate-mark-inversion (AMI) or pseudo-return-to-zero (PRZ), which can be exploited for clock recovery, has been demonstrated by various technologies including the use of the gain saturation effect of a semiconductor optical amplifier (SOA)[1−3], an asymmetric Mach-Zehnder interferometer[4,5], and self-phase modulation in a Fabry-Pérot laser diode[6,7]. However, all these schemes are disadvantageous in large device footprint, thus render themselves unfavorable for compact photonic integrated circuits in practical applications.

Recently, silicon microring resonator devices, which can be fabricated by the mature complementary metal oxide semiconductor (CMOS) compatible processes facilitate integration, have attracted a lot of interests for optical signal processing applications[8−11]. In Ref. [12], a silicon second-order coupled-microring resonator was introduced to perform 3.6-Gbps format conversion from NRZ to PRZ. However, as the results shown in Ref. [12], the amplitude of PRZ signal fluctuates severely.

In this letter, we use a silicon resonator containing a single microring to perform the 10-Gbps NRZ-to-AMI conversion in experiment, which is the highest rate of such conversion to date. The operation principle is based on the linear filtering effect provided by the silicon ring resonator. In the frequency domain, the carrier of the NRZ signal is suppressed and correspondingly the optical clock component is enhanced by the notch filter. Therefore, in the time domain, the signal after the silicon ring resonator exhibits discrete AMI pulses positioned in the transition edges of the NRZ signals[12]. We also analyze the dependence of the quality of AMI signal on the notch depth and 3-dB bandwidth of the resonance in simulation, which shows that a 10-Gb/s AMI signal with a good signal quality can be obtained by a microring resonator with a notch depth larger than 25 dB when the 3-dB bandwidth is 0.4 nm.

The microring resonator employed in this work is fabricated in a commercial silicon-on-insulator (SOI) wafer with a 3-μm-thick silica buffer and a 250-nm crystalline silicon top layer in the Royal Institute of Technology of Sweden. The radius of the ring is 40 μm. The waveguide cross-section is 450 × 250 (nm). The air gap between the waveguide and the ring is controlled at 120 nm to approach critical coupling. The scanning electron microscope (SEM) photo is shown in Fig. 1(a). The waveguide is slowly tapered to a width of 10 μm at both ends,

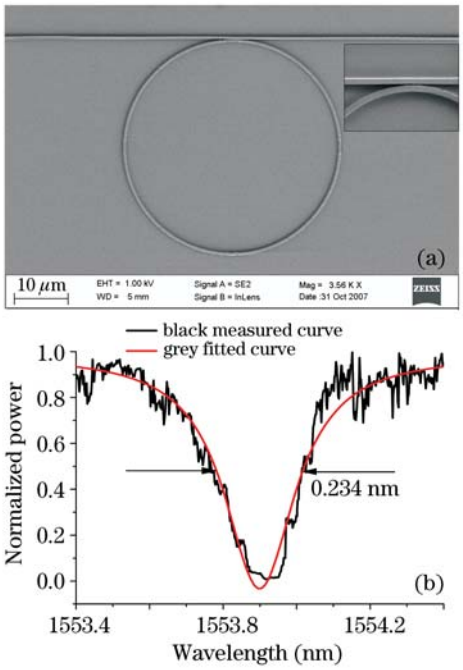

Fig. 1. (a) SEM photos of the SOI 40-μm-radius micro-ring resonator, and (b) spectrum of the resonance at 1549.80 nm. Inset in (a) is a zoom-in view of the coupling region.

and then gold gratings are added to couple light near-vertically from single mode fibers[13]. The spectral response of the microring resonator is shown in Fig. 1(b). The black and gray curves denote the measured and Lorentzian fitted resonance, respectively. The resonance at 1553.900 nm has a 20-dB notch and the 3-dB bandwidth is about 0.234 nm. Therefore, the Q factor of this resonance is about 6640 and the estimated total loss is about 10 dB/cm. The total loss comprises the transmission loss and the bending loss. The propagation loss is mostly affected by the sidewall roughness while the bending loss increases significantly as bending radius decreases. Generally speaking, the bending loss dominates the total loss for small bending radius (< 5 μm)[14,15]. Another related loss is the coupling loss between the fiber and the waveguide, which results from the large mode size mismatch. In our experiment, we use the vertical coupling system to couple the light into the microring resonator and the coupling loss is around 20 dB. However, this value can be significantly reduced to below 2 dB by inverted-taper mode converter[16].

The experimental setup is depicted in Fig. 2. The tunable laser (TSL-210F, Santec, Japan), which has a wide tuning range from 1260 to 1630 nm and a tuning resolution of 0.001 nm, is tuned at the resonance wavelength of 1553.900 nm. The laser output is modulated by a Mach-Zehder modulator (MZM), which is biased at the quadrature point and driven by a 10-Gb/s electrical pseudo-random-binary-signal (PRBS) signal of $2^7 - 1$ pattern length. The generated NRZ signal is then coupled into the microring resonator by the vertical coupling system. As the gold grating coupler is polarization-dependent, a polarization controller (PC) is inserted before the grating to make sure that the input signal is in transverse-electric (TE) mode. Two cascaded erbium-doped fiber amplifiers (EDFAs) after the resonator are used to compensate the coupling loss. The waveforms of the input NRZ signal and the converted AMI signal are recorded by the oscilloscope (83430A, Hewlett-Packard, USA) with an optical bandwidth of 20 G. The input power before the grating is around 0 dBm and the estimated power into the microring resonator is -10 dBm.

Figures 3(a) and (b) depict the waveforms of the input NRZ data and the converted AMI data, respectively. Sharp pulses of AMI data appear at both the rising and falling edges in "1" bits of NRZ data due to the effective suppression of the optical carrier and thus enhancement of the optical clock component in the notch filter transmission. The AMI data has a pulse width of about 32 ps and provides well-defined 10-Gb/s clock information. However, it can be seen from Fig. 3(b) that the amplitude

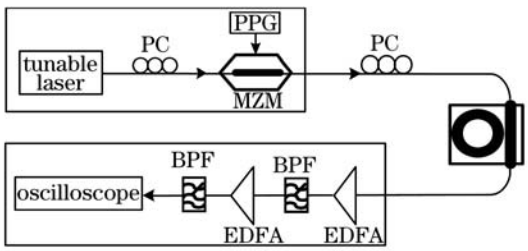

Fig. 2. Experimental setup for the NRZ-to-AMI format conversion. PPG: pulse pattern generator; BPF: bandpass filter.

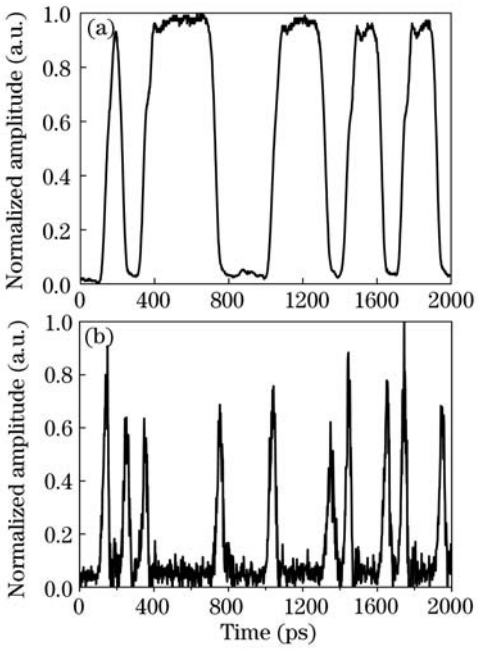

Fig. 3. (a) and (b) are experimental waveforms of the input NRZ signal and the converted AMI signal, respectively.

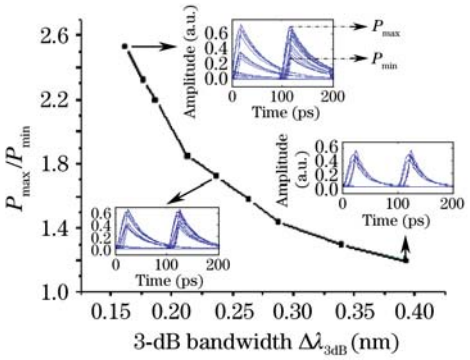

Fig. 4. Simulation results of the dependence of $P_{\max}/P_{\min}$ on the $\Delta\lambda_{3\mathrm{dB}}$ of the resonance at a notch depth of 30 dB. Insets are the eye diagrams at $\Delta\lambda_{3\mathrm{dB}} = 0.15$, 0.23, and 0.4 nm, respectively.

of the pulse train exhibits certain fluctuation, which is similar to the results in Ref. [12]. The following sections will analyze through simulations such fluctuations, which can be suppressed if the 3-dB bandwidth and the notch depth of the microring resonator are carefully designed.

To characterize the fluctuations of the AMI pulses, we define $P_{\max}/P_{\min}$ as a fluctuation factor, where the $P_{\max}$ and $P_{\min}$ are the maximal and minimal amplitudes, respectively. Figure 4 investigates the dependence of $P_{\max}/P_{\min}$ on the 3-dB bandwidth of the ring resonance with the notch depth fixed in simulation. The result displays that the fluctuation factor decreases as the 3-dB bandwidth $\Delta\lambda_{3\mathrm{dB}}$ increases, which is also verified by the eye diagrams shown in the insets. The reason is that more frequency components close to the optical carrier are removed when the $\Delta\lambda_{3\mathrm{dB}}$ becomes larger, which in turn enhances the clock component of the signal. However, the amplitude of AMI signal is reduced correspondingly with larger 3-dB bandwidth. Therefore, a balance is needed.

On the other hand, Fig. 5 compares the eye diagrams of

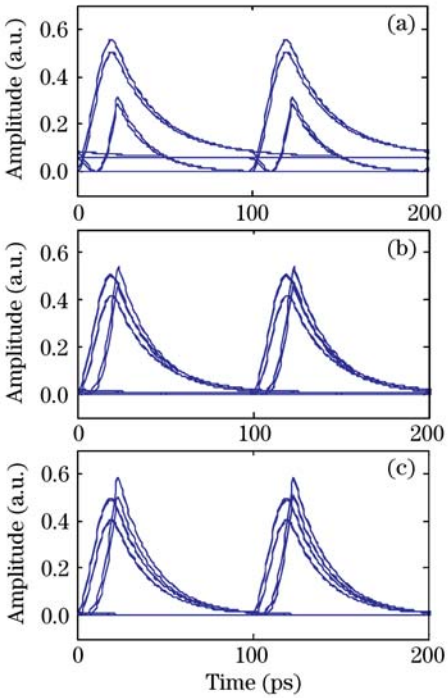

Fig. 5. Simulation results of the eye diagrams of AMI signal corresponding to a notch depth of (a) 12.4, (b) 27.2, and (c) 40 dB, respectively. The resonance bandwidth is fixed at 0.4 nm.

AMI signal at different notch depths with the 3-dB bandwidth fixed at 0.4 nm in simulation. It demonstrates that the eye-opening becomes wider with the increase of the notch depth. In particular, wide eye-opening can be obtained if the notch depth of the microring resonator is larger than 25 dB.

In summary, we demonstrated the 10-Gb/s all-optical NRZ to AMI format conversion using the linear filtering effect of a silicon microring resonator in experiment. However, the converted AMI signal exhibits certain fluctuation in its amplitude. To obtain an AMI data with a good signal quality, we investigate the dependence of amplitude fluctuation on the notch depth and 3-dB bandwidth of the ring resonance in simulation. Our simulation results conclude that a 10-Gb/s AMI signal with a good signal quality can be obtained by a resonator with a notch depth larger than 25 dB when the 3-dB bandwidth is around 0.4 nm.

This work was supported by the National Natural Science Foundation of China (No. 60777040), the National "863" Project of China (No. 2006AA01Z255), Shanghai Rising Star Program Phase II (No. 07QH14008), and the Fok Ying Tung Fund (No. 101067). Z. Zhang and M. Qiu thank the supports from the Swedish Foundation for Strategic Research (SSF) through the future research leader program, and from the Swedish Research Council (VR).

References

1. P. E. Barnsley, Electron. Lett. **28,** 1253 (1992).
2. H. J. Lee, H. G. Kim, J. Y. Choi, and H. K. Lee, Electron. Lett. **35,** 989 (1999).
3. H. J. Lee and C. S. Park, Opt. Commun. **181,** 323 (2000).
4. C. H. Lee and H. K. Lee, in *Proceedings of LEOS 1996* **2,** 113 (1996).
5. H. K. Lee, C. H. Lee, S. B. Kang, M. Y. Jeon, K. H. Kim, J. T. Ahn, and E. H. Lee, Electron. Lett. **34,** 478 (1998).
6. Y. D. Jeong, H. J. Lee, H. Yoo, and Y. H. Won, IEEE Photon. Technol. Lett. **16,** 1179 (2004).
7. Y. C. Chang, Y. H. Lin, J. H. Chen, and G. R. Lin. Opt. Express **12,** 4449 (2004).
8. T. Ye, F. Liu, and Y. Su, Chin. Opt. Lett. **6,** 398 (2008).
9. A. Fojtik, J. Valenta, I. Pelant, M. Kalal, and P. Fiala, Chin. Opt. Lett. **5,** 250 (2007).
10. Z. Li, J. Yu, S. Chen, J. Liu, and J. Xia, Chin. Opt. Lett. **5,** 215 (2007).
11. Z. Zhang, M. Qiu, U. Andersson, and L. Tong, Chin. Opt. Lett. **5,** 577 (2007).
12. L. Zhou, H. Chen, and A. W. Poon. in *Proceedings of LEOS 2007, CLEO 2007* 1 (2007).
13. S. Scheerlinck, J. Schrauwen, F. Van Laere, D. Taillaert, D. Van Thourhout, and R. Baets. Opt. Express **15,** 9625 (2007).
14. F. Xia, L. Sekaric, and Y. Vlasov, Nature Photon. **1,** 65 (2007).
15. F. Xia, L. Sekaric, M. O'Boyle, and Y. A. Vlasov, Appl. Phys. Lett. **89,** 041122 (2006).
16. Y. Vlasov, W. M. J. Green, and F. Xia, Nature Photon. **2,** 242 (2008).